Biochemical and Biophysical Research Communications 426 (2012) 533–538

Contents lists available at SciVerse ScienceDirect

Biochemical and Biophysical Research Communications

journal homepage: www.elsevier.com/locate/ybbrc

Similar phenotypes of Girdin germ-line and conditional knockout mice indicate a crucial role for *Girdin* in the nestin lineage

Masato Asai [a,b,*], Naoya Asai [a,d], Ayana Murata [a], Hirofumi Yokota [a], Kenji Ohmori [a,c], Shinji Mii [a], Atsushi Enomoto [a], Yoshiki Murakumo [a], Masahide Takahashi [a,d,*]

[a] Department of Pathology, Nagoya University Graduate School of Medicine, 65 Tsurumai-cho, Showa-ku, Nagoya 466-8550, Japan
[b] Department of Endocrinology and Diabetes, Nagoya University Graduate School of Medicine, 65 Tsurumai-cho, Showa-ku, Nagoya 466-8550, Japan
[c] Division of Surgical Oncology, Department of Surgery, Nagoya University Graduate School of Medicine, 65 Tsurumai-cho, Showa-ku, Nagoya 466-8550, Japan
[d] Division of Molecular Pathology, Center for Neurological Disease and Cancer, Nagoya University Graduate School of Medicine, 65 Tsurumai-cho, Showa-ku, Nagoya 466-8550, Japan

ARTICLE INFO

Article history:
Received 10 August 2012
Available online 4 September 2012

Keywords:
Girdin
Neuronal migration
Granule cell dispersion
RMS
Nestin

ABSTRACT

Girdin is an Akt substrate and actin-binding protein. Mice with germ-line deletions of Girdin (a non-conditional knockout, (ncKO)) exhibit complete postnatal lethality accompanied by growth retardation and neuronal cell migration defects, which results in hypoplasia of the olfactory bulb and granule cell dispersion in the dentate gyrus. However, the physiological and molecular abnormalities in Girdin ncKO mice are not fully understood. In this study, we first defined the distribution of Girdin in neonates (P1) and adults (6 months or older) using β-galactosidase activity in tissues from ncKO mice. The results indicate that Girdin is expressed throughout the nervous system (brain, spinal cord, enteric and autonomic nervous systems). In addition, β-galactosidase activity was detected in non-neural tissues, particularly in tissues with high tensile force, such as tendons, heart valves, and skeletal muscle. In order to identify the cellular population where the Girdin ncKO phenotype originates, newly generated Girdin flox mice were crossed with nestin promoter-driven Cre transgenic mice to obtain Girdin conditional knockout (cKO) mice. The phenotype of Girdin cKO mice was almost identical to ncKO mice, including postnatal lethality, growth retardation and decreased neuronal migration. Our findings indicate that loss of Girdin in the nestin cell lineage underlies the phenotype of Girdin ncKO mice.

1. Introduction

Our group identified an actin binding protein Girdin (girder of actin filament) (also known as APE, GIV, HkRP1) as a binding partner of Akt/PKB, which plays crucial roles in the migration of fibroblasts, cancer cells, endothelial cells and neuronal cells [1–4]. Mice with a germ-line deletion of Girdin (ncKO) exhibit hypoplasia of the olfactory bulb (OB) with a widened rostral migratory stream (RMS) and granule cell dispersion (GCD) in the dentate gyrus [4]. Girdin ncKOs also exhibited postnatal growth retardation and pre-weaning lethality [2]. Cross-explant experiments with Girdin +/+ and −/− mice showed that the neuronal migration defect is cell-autonomous [5]. We found that Girdin is essential for neuronal migration from the subventricular zone (SVZ) of the lateral ventricles and from the subgranular zone (SGZ) of the dentate gyrus. However, the defects that cause the Girdin ncKO phenotype are not fully understood.

Postnatal neuronal migration in the murine brain occurs at two major sites, the SVZ and the SGZ [6], where abnormalities were found in Girdin ncKO mice. Neurons born in the SVZ migrate through the RMS to supply the OB with GABAergic neurons, while neurons born in the adult SGZ migrate into the granule cell layer of the dentate gyrus [6,7]. One typical manifestation of migration defects in SVZ neurons is hypoplasia of the OB with a widened RMS, presumably due to positioning failure and a shortage of neurons migrating into the OB. On the other hand, a migration defect in SGZ neurons results in granule cell dispersion (GCD), which was first reported in 1990 [8] and is often associated with human mesial–temporal lobe epilepsy (MTLE) [9]. An MTLE-like phenotype was also observed in Girdin mutant mice (data not shown).

In this study, to determine the cellular populations where Girdin functions, we first performed a histological survey of Girdin expression using β-galactosidase staining of tissues of ncKO mice. Secondly, we generated Girdin conditional knockout (cKO) mice using the Cre/loxP system, and removed Girdin in cells of the nestin lineage. Girdin cKO mice exhibited almost identical phenotype to that of Girdin ncKO mice.

* Corresponding authors at: Department of Pathology, Nagoya University Graduate School of Medicine, 65 Tsurumai-cho, Showa-ku, Nagoya 466-8550, Japan. Fax: +81 52 744 2098.
E-mail addresses: Masato-a@med.nagoya-u.ac.jp (M. Asai), mtakaha@med.nagoya-u.ac.jp (M. Takahashi).

0006-291X/$ - see front matter © 2012 Elsevier Inc. All rights reserved.
http://dx.doi.org/10.1016/j.bbrc.2012.08.122

2. Materials and methods

2.1. Girdin ncKOs and Girdin flox mice

Generation of Girdin ncKOs was previously described [2]. Briefly, a β-galactosidase (LacZ)-PGK-neo cassette was inserted five amino acids downstream of the start codon of the mouse Girdin gene using homologous recombination of the gene-targeting vector. After *in vivo* excision of the floxed PGK-neo cassette, the nuclear localization signal (NLS)-containing β-galactosidase gene was expressed under the control of the Girdin gene promoter [2].

Girdin flox mice were generated using a newly created vector containing a floxed mouse Girdin exon 3 preceded by a flippase recognition target (FRT) -flanked PGK-neo cassette. After *in vivo* removal of the PGK-neo cassette, floxed mouse Girdin exon 3 becomes vulnerable to Cre-excision. Deletion of exon 3 (109 bp) causes translation of an aberrant protein due to a premature stop codon. Mice carrying nestin promoter-driven Cre (nestin-Cre mice; strain name, B6.Cg-Tg(Nes-cre)1Kln/J; stock number: 003771) were obtained from the Jackson Laboratory (Bar Harbor, ME, USA). *Girdin*$^{+/flox}$; nestin-*Cre*(+) mice were mated with *Girdin*$^{flox/flox}$; nestin-*Cre*(−) mice to maintain a closed colony. The genetic background of the mice was mixed C57Bl/6 and 129 sv/J. The Animal Care and Use Committee of Nagoya University Graduate School of Medicine approved all animal protocols.

2.2. β-Galactosidase staining

β-Galactosidase staining was performed as described previously [10]. Briefly, mice were perfused with phosphate-buffered saline (PBS), fixative (PBS/2 mM $MgCl_2$, 0.2% glutaraldehyde, 50 mM ethylene glycol tetraacetic acid, pH7.3), and 30% sucrose in PBS. Dissected tissues from adult mice or the whole body of postnatal day 1 (P1) mice were soaked in the same fixative for 30 min on ice, 30% sucrose in PBS overnight at 4 °C, and cryosectioned at 10 μm. Slides were stained in β-galactosidase staining buffer (PBS/2 mM $MgCl_2$, 0.01% sodium deoxycholate, 0.02% Igepal, 5 mM potassium ferrocyanide, 5 mM potassium ferricyanide, 0.5 mg/ml 5-bromo-4-chloro-3-indolyl-β-D-galactoside (X-gal, Wako, Aichi, Japan)) for 48 h at 37 °C. Stained slides were postfixed in 4% PFA, and counter-stained with eosin.

2.3. Immunohistochemistry (IHC)

Methods for IHC have been previous described [5]. Briefly, mice were perfused with 4% paraformaldehyde (PFA) and the brain was removed. Dissected brain tissue was postfixed in 4% PFA overnight, then sectioned at 50 μm using a microslicer (VT1200S; Leica Microsystems). Free-floating sections were incubated in 1% hydrogen peroxide in PBS for 20 min, and in serum free Protein block (Dako, Glostrup, Denmark) for 15 min. The sections were then incubated with anti-Doublecortin antibody (1:100 dilution, sc-8066 Santa Cruz Biotechnology, Santa Cruz, CA, USA) for 2 days at 4 °C, followed by incubation with anti-goat IgG antibody conjugated with biotin (1:500 dilution, 705-065-147 Jackson Immuno Research, West Grove, PA, USA), and HRP-streptavidin (1:500 dilution, SA-5004, Vector, Burlingame, CA, USA) for 30 min at RT. Signal detection was performed using DAB color reaction substrate (K3488, Dako). For β-galactosidase/IHC double staining, whole-mount β-galactosidase staining was carried out as described previously [10], followed by paraffin embedding, sectioning and IHC using anti-microtubule-associated protein 2 (MAP2) antibody (clone 5F9, Upstate, East Syracuse, NY, USA), or anti-glial fibrillary acidic protein (GFAP) antibody (clone 6F2, Dako).

2.4. Southern Blot analysis, PCR genotyping, RT-PCR, subcloning and sequencing

Detailed protocols are described in supplementary information.

3. Results

3.1. Distribution of Girdin-driven β-galactosidase expression

Girdin ncKO mice exhibited postnatal growth retardation and pre-weaning lethality with neural phenotype (OB hypoplasia and GCD in the dentate gyrus) [1,2]. To elucidate which population of mutant cells is the source of the phenotype, it is important to characterize the Girdin expression profile at all stages of life. Previous studies have demonstrated that Girdin is expressed in multiple tissues including muscle, kidney, lung, heart, testis, adipose tissue, brain, and spleen in adult mice [1,11–13]. However, histological information on the distribution of Girdin throughout the body in postnatal mouse is not available. To investigate the precise distribution of Girdin expression, we performed β-galactosidase staining of tissues of Girdin ncKO mice, in which the Girdin coding sequence was replaced with a β-galactosidase (*LacZ*) gene under the control of the Girdin promoter [4], at two representative time points (P1 and adults older than 6 months).

Our results indicate that Girdin expression is not limited to the tissues that express a phenotype, namely the OB, RMS and the dentate gyrus. Girdin-driven β-galactosidase activity was also detected in other brain regions including the cerebral cortices (frontal association cortex, motor cortex, somatosensory cortex, piriform cortex, and visual cortex), caudate putamen, cornu ammonis (CA) fields 1 and 3, the olfactory tubercle, subiculum, triangular septal nucleus, habenular nucleus, pontine nuclei, superior colliculus, and the cerebellum (Fig. 1). β-Galactosidase-positive cells in the glomerular layer of the OB co-stained with a neuronal marker, microtubule-associated protein 2 (MAP2), but not with glial fibrillary acidic protein (GFAP) (Supplementary Fig. 1), suggesting that Girdin is expressed mainly in neurons, not in mature astrocytes.

In contrast to the broad expression of Girdin-driven β-galactosidase activity in adult brain, activity in P1 brains was detected in more limited regions, including the caudate putamen, SVZ, RMS, and the OB, which may imply that Girdin functions primarily during postnatal stages of brain development (Supplementary Fig. 2).

β-Galactosidase activity was also observed in other regions of the central nervous system (CNS) and in the peripheral nervous system (PNS); however, the distribution was not as widespread as previously reported. Girdin-driven β-galactosidase positive tissues in the adult CNS included the spinal cord and retina. In the PNS, we detected β-galactosidase activity in the dorsal root ganglia (DRG), sympathetic ganglia, and in enteric neurons (Supplementary Fig. 3). In addition, expression was detected in non-neural tissues of the adult, such as the pelvic tendon, skeletal muscle, heart valves, vessels, and the seminiferous tubules of the testes (Supplementary Fig. 3). The distribution of Girdin β-galactosidase activity in non-neural tissues at P1 was similar to that of adult mice with two exceptions: considerable activity in subcutaneous mesenchymal cells was observed only at P1 and intense activity in the testes was detected only in adult mice (Supplementary Figs. 3 and 4).

3.2. Generation of Girdin flox mice

In order to better understand the phenotype of Girdin ncKO mice, we generated Girdin flox mice using DNA homologous recombination (Fig. 2A). Mouse Girdin exon 3 was selected to flox, because its excision (109 bp) causes a frame shift and generates a premature stop codon. An FRT-flanked PGK-neo cassette was used

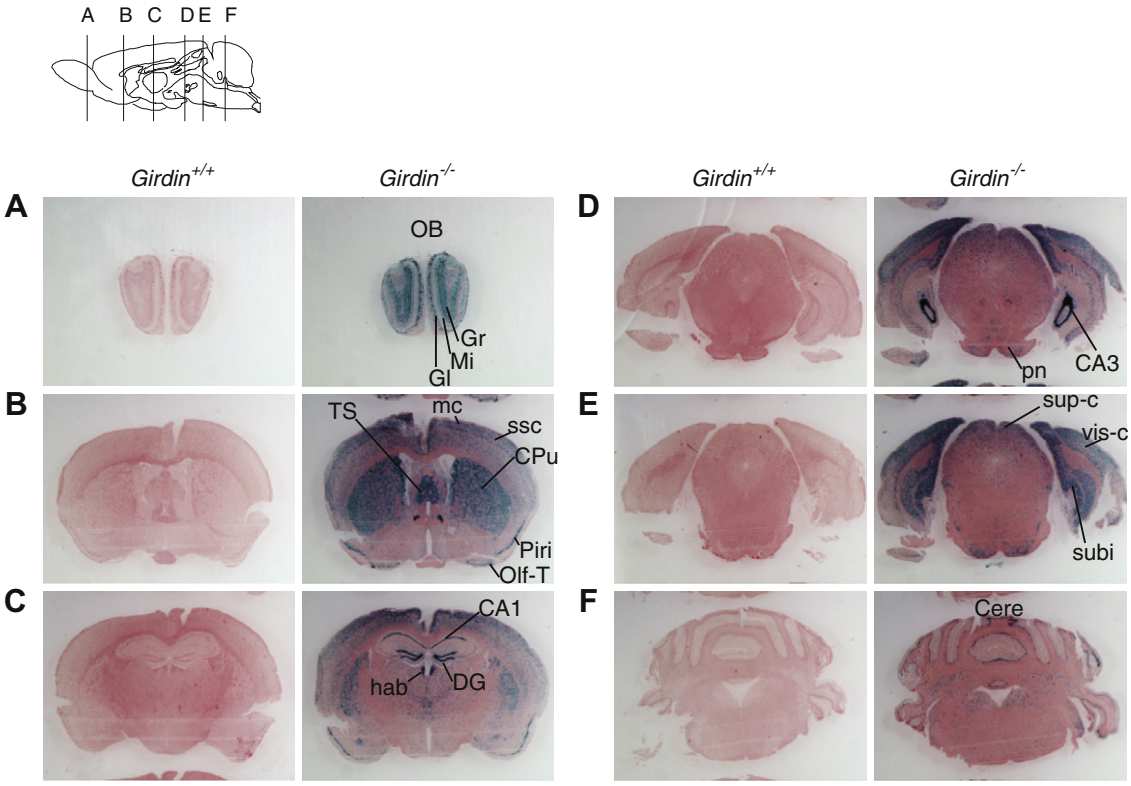

Fig. 1. Histological analysis of Girdin expression in the adult mouse brain. Ten μm coronal cryosections of adult (6 months or older) WT (Girdin$^{+/+}$, left panels) or heterozygous Girdin ncKO (Girdin$^{+/-}$, right panels) mice after β-galactosidase staining and eosin counter-staining. Positive signals are blue stained nuclei due to the NLS encoded in the β-galactosidase construct. The top-left illustration indicates the section level of the brain for panels A–F. Wild type mice were stained as a control for endogenous β-galactosidase activity. Strong Girdin-driven β-galactosidase activity was observed in the olfactory bulb (OB), caudate putamen (CPu), dentate gyrus (DG), olfactory tubercle (Olf-T), motor cortex (mc), somatosensory cortex (ssc), triangular septal nucleus (TS), piriform cortex (piri), habenular nucleus (hab), cornu ammonis field 1 (CA1), cornu ammonis field 3 (CA3), pontine nuclei (pn), superior colliculus (sup-c), visual cortex (vis-c), subiculum (subi), and cerebellum (cere). Gr, granular cell layer; Mi, mitral cell layer; Gl, glomerular layer.

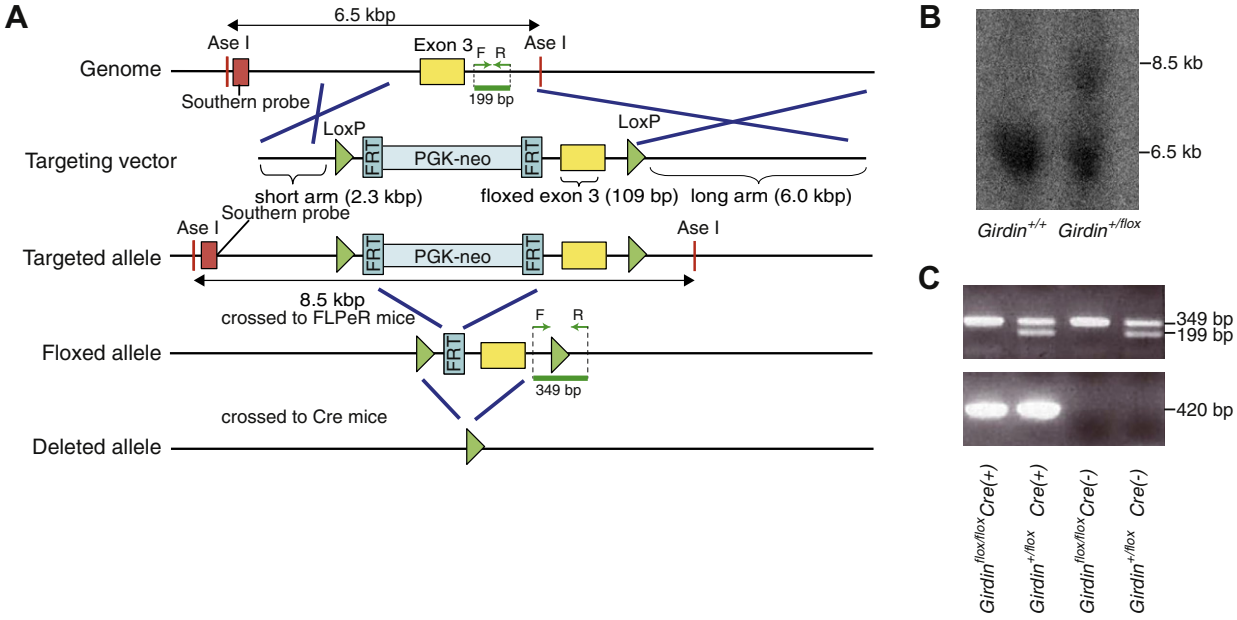

Fig. 2. Generation of Girdin flox mice. (A) The targeting vector contains a PGK-driven neo (PGK-neo) cassette flanked by homologous genomic DNA containing Girdin exon 3. The PGK-neo cassette was removed by crossing heterozygous neo mice with Flippase-expressing mice. Light green arrows in the genome indicate the locations of genotyping primers (F, forward primer; R, reverse primer). (B) Incorporation of the targeting construct into genomic DNA was confirmed by Southern Blot analysis. DNA extracted from ES cells was digested with Ase I restriction endonuclease, transferred, and hybridized with the probe indicated in A. The 8.5 kb band is the floxed allele, the 6.5 kb band is the WT allele. (C) Genotyping of animals by PCR. Upper panel: The WT (199 bp band) and floxed (349 bp band) alleles are shown. Lower panel: the 420 bp band shows the presence of hemizygous nestin-Cre.

to select transfected ES cells. After obtaining F1 neo mice, the PGK-neo cassette was removed by crossing to flippase (FLPeR) mice. Incorporation of the targeting vector was confirmed using Southern Blot analysis (Fig. 2B). An 8.5 kb Ase I fragment indicates that the Girdin allele was correctly targeted. To genotype the mice we used PCR to discriminate between the *Girdin*$^{flox/flox}$ (a single 349 bp band) and *Girdin*$^{+/flox}$ (two bands of 349 and 199 bp) mice and the *nestin-Cre*(+) (a single 420 bp band) and *nestin-Cre*(−) (no band) mice (Fig. 2C). We thus confirmed that the Girdin flox mice were generated as we designed.

Given that Girdin is highly expressed in the nervous system, we generated cKO mice using nestin-Cre transgenic mice, which results in Girdin deletion only in the nestin cell lineage. Nestin is a widely-accepted neural stem cell marker [14]. To obtain Girdin cKO mice (*Girdin*$^{flox/flox}$; *Cre*(+)), *Girdin*$^{+/flox}$; *Cre*(+) mice and *Girdin*$^{flox/flox}$; Cre(−) mice were mated to generate four possible genotypes; *Girdin*$^{+/flox}$; *Cre*(−), *Girdin*$^{flox/flox}$; *Cre*(−), *Girdin*$^{+/flox}$; *Cre*(+), and *Girdin*$^{flox/flox}$; *Cre*(+). To validate the deletion of exon 3 in the cKOs, we designed an RT-PCR primer pair that amplified both excised and floxed (non-excised) exon 3 (floxed allele, 262 bp; excised allele, 153 bp (Fig. 3A)). The integrity of Girdin mRNA expression in the whole brain was monitored using RT-PCR primers that span introns 21–22 (Fig. 3A, right lower panel).

RT-PCR was performed using RNA from P15 brains of all four genotypes, and the expected excision was confirmed by the presence of a 153 bp band in the *Girdin*$^{flox/flox}$; *Cre*(+) and *Girdin*$^{+/flox}$; *Cre*(+) samples (Fig. 3A, right upper panel). In *Girdin*$^{flox/flox}$; *Cre*(+) samples, only the 153 bp band was visible, which suggests that in almost all cells that express nestin-Cre, both Girdin exon 3 alleles were excised from the genome. In contrast, a 153 bp band was not amplified from nestin-Cre negative tissues in mice of any genotype (data not shown). The sequence of the 153 bp band from *Girdin*$^{flox/flox}$; *Cre*(+) mice contained an exon2/exon4 junction in Girdin, which causes a frame shift and results in a premature stop codon following six aberrant amino acids. The sequence of the 262 bp fragment amplified from *Girdin*$^{flox/flox}$; *Cre*(−) mice contained an unaltered Girdin mRNA fragment (Fig. 3B). These findings clearly demonstrate that Girdin flox mice serve as a functional Girdin cKO when crossed with nestin-Cre mice.

3.3. Phenotype of mice lacking Girdin in the nestin lineage

Abnormalities of Girdin ncKO mice (OB hypoplasia with a widened RMS, GCD in the dentate gyrus, growth retardation, and postnatal lethality) are transmitted as a recessive trait [5]. The cKO mice (*Girdin*$^{flox/flox}$; *Cre*(+)) were viable. The expected Medelian ratio of each genotype (*Girdin*$^{+/flox}$; *Cre*(−), *Girdin*$^{flox/flox}$; *Cre*(−), *Girdin*$^{+/flox}$; *Cre*(+), and *Girdin*$^{flox/flox}$; *Cre*(+)) was 1:1:1:1. Actual numbers of births of *Girdin*$^{+/flox}$; *Cre*(−), *Girdin*$^{flox/flox}$; *Cre*(−), *Girdin*$^{+/flox}$; *Cre*(+), and *Girdin*$^{flox/flox}$; *Cre*(+) were 62, 53, 69, and 58, respectively. Chi-square tests of observed and expected births did not exhibit a statistically significant difference ($p = 0.132$), which suggests the absence of embryonic lethality in *Girdin*$^{flox/flox}$; *Cre*(+) mice. Although no external malformations were observed in cKO mice at birth, the body weight of pups tended to be slightly lighter than those of other genotypes ($p = 0.038$ at P0 for ANOVA) from P5 onwards ($p < 0.001$) (Fig. 4A). Additionally, no cKOs were successfully weaned. The cKO mice were inactive, and exhibited growth retardation and fatality after P12, with none surviving past P29

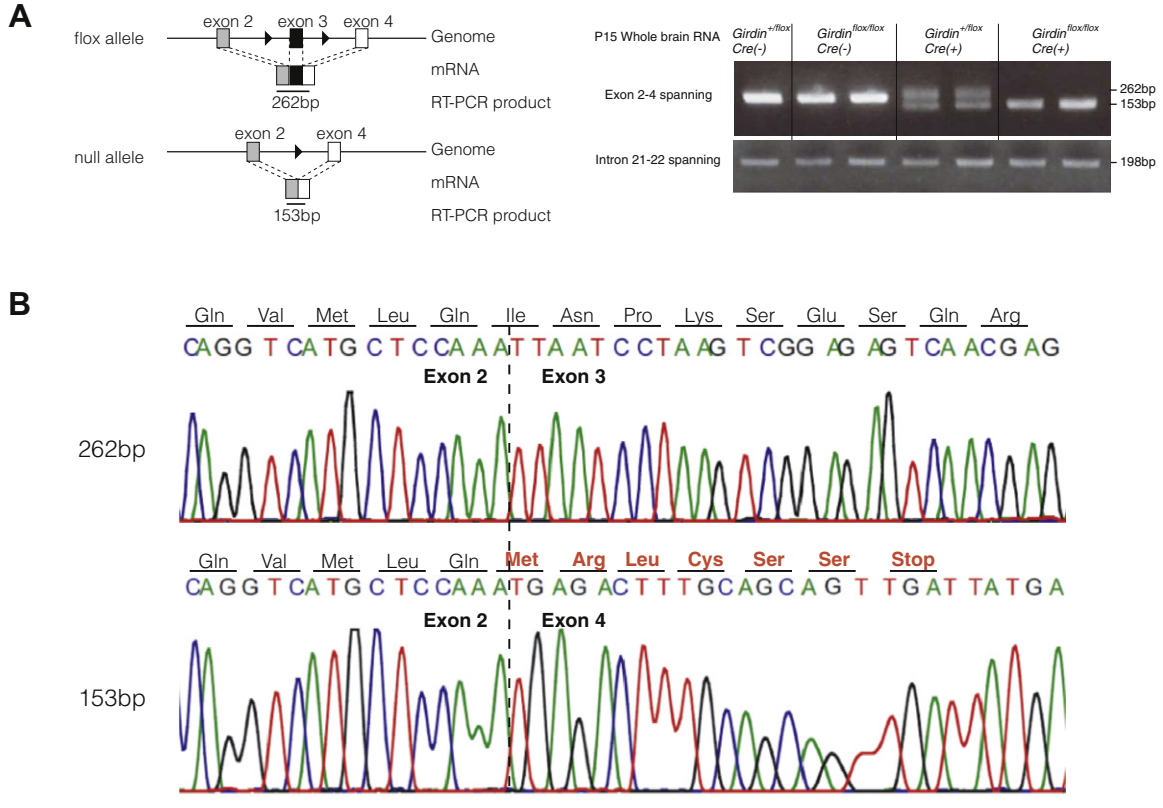

Fig. 3. Validation of Girdin$^{flox/flox}$; nestin-Cre(+) mice. (A) (Left panel) Boxes represent relative locations of mouse *Girdin* exons 2–4. Black triangles indicate loxP sites (flox allele, top; null allele, bottom) for exon 3 excision (109 bp). Sizes of expected RT-PCR products using primers spanning Girdin exons 2–4: flox allele, 262 bp; null allele, 153 bp. (Right panel) Whole brain RT-PCR results of P15 mice of four genotypes. cDNA was amplified for 35 cycles using primers spanning Girdin exons 2–4. In "*Girdin*$^{flox/flox}$; *Cre*(+)" lanes, only the 153 bp bands are visible. (B) Sequence chromatograms of the 262 bp band from *Girdin*$^{flox/flox}$; *Cre*(−) mice ("262 bp", upper chromatogram and translation) and the 153 bp band from *Girdin*$^{flox/flox}$; *Cre*(+) mice ("153 bp", lower chromatogram) containing the 3' end of exon 2. The 153 bp band contains an exon 2/exon 4 junction, which causes a frame shift and premature stop codon (lower translation).

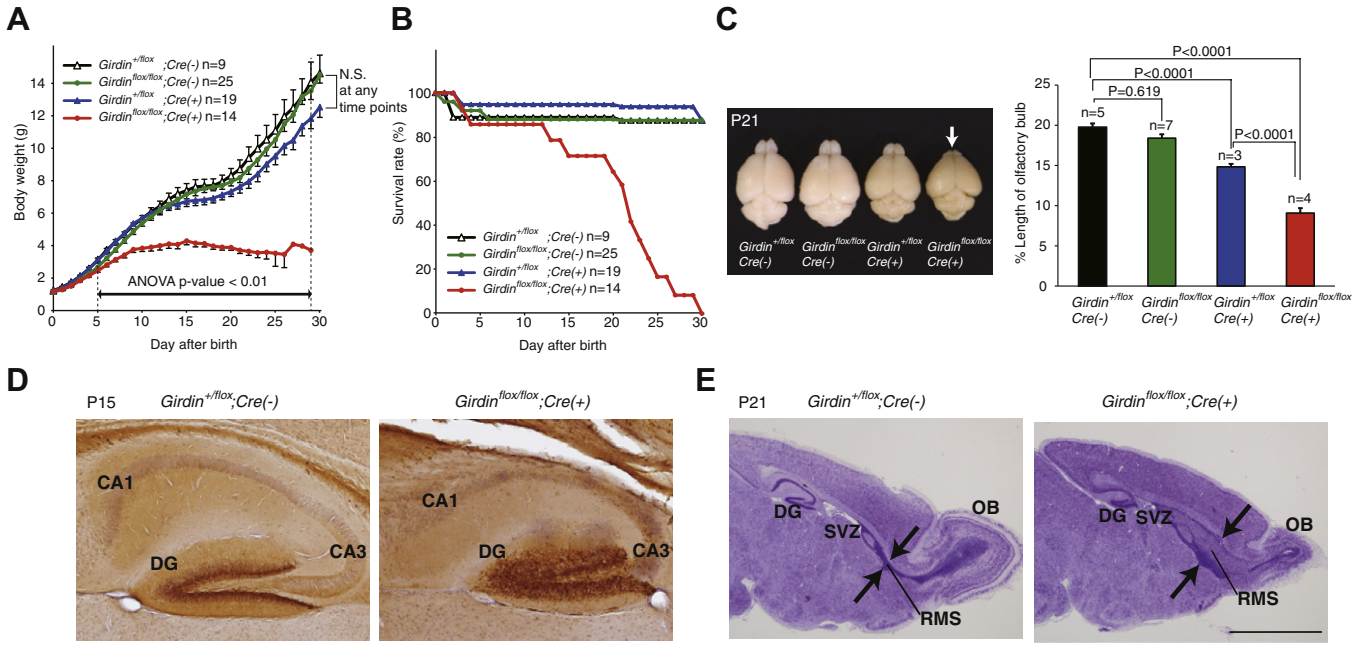

Fig. 4. Phenotype of *Girdin* cKO mice. (A, B) Body weights (panel A) and survival rates (panel B) of *Girdin*$^{+/flox}$; *Cre*(−), *Girdin*$^{flox/flox}$; *Cre*(−), *Girdin*$^{+/flox}$; *Cre*(+), and *Girdin*$^{flox/flox}$; *Cre*(+) mice. (C) Girdin cKOs exhibit OB hypoplasia. (Left) P21 brains of four genotypes (male mice) were photographed. The % length of the OB was defined as a percentage of the distance from the anterior tip of the bulb to the anterior edge of the cerebral hemisphere in relation to the distance from the anterior tip of the bulb to the posterior edge of the cerebellum. Girdin cKOs exhibit OB hypoplasia (white arrow). (Right) *Post hoc* Bonferroni's method was applied to calculate *p*-values. The difference was significant if the *p*-value was less than 0.0083. (D) Girdin cKOs exhibit granule cell dispersion (GCD). Immunohistochemistry of 50 μm sections of P15 mouse brains using anti-Doublecortin antibodies. (Left), *Girdin*$^{+/flox}$; *Cre*(−); (Right), *Girdin*$^{flox/flox}$; *Cre*(+). Dcx-positive neurons were dispersed and irregularly aligned in the dentate gyrus of Girdin cKO mice. CA1, CA3, cornu ammonis fields 1 and 3 of the hippocampus; DG, dentate gyrus. (E) Girdin cKOs exhibit a widened rostral migratory stream (RMS). Nissl staining of sagittal sections of P21 mouse brains. Girdin cKOs exhibit a widened RMS. (Left), *Girdin*$^{+/flox}$; *Cre*(−); (Right), *Girdin*$^{flox/flox}$; *Cre*(+). OB, olfactory bulb; DG, dentate gyrus; SVZ, subventricular zone. Scale bar, 2 mm.

(Fig. 4B). In contrast, survival among the three other genotypes was typically longer than one year (data not shown).

Dead cKO mice were usually underweight, suggesting the involvement of malnutrition in the cause of death, although we could not find any fundamental cause of malnutrition. No abnormalities were observed in suckling or motor behavior. Neither ataxia nor intestinal dilation was observed. No morphological abnormalities were detected in other digestive organs (teeth, tongue, oral cavities, and intestines). There were no sex differences in cKO mice in any of phenotype (data not shown). Macroscopically, the average longitudinal length of the cKOs' OBs was extremely smaller than in mice of other genotypes. The size reduction of the OB was disproportionate to the reduction of the whole brain (Fig. 4C). Less severe but significant size reduction in the OB was also observed in *Girdin*$^{+/flox}$; *Cre*(+) mice (Fig. 4C).

The characteristic abnormality in the granule cell layer of the dentate gyrus was also observed in cKO mice. Immunohistochemisty in the dentate gyrus using anti-Doublecortin (DCX) antibodies revealed an increased width of the layer of DCX-positive neurons of P15 cKO mice, compared with *Girdin*$^{+/flox}$; *Cre*(−) mice of the same age (Fig. 4D). In addition, Nissl staining of sagittal sections of P21 brain showed a widened RMS in cKO mice (Fig. 4E). These structural abnormalities in the OB and the dentate gyrus seemed essentially identical to previously reported phenotype of Girdin ncKO mice [4,5]. Thus, we confirmed that ablation of Girdin in the nestin cell lineage creates cKO mice with phenotype that are indistinguishable from those seen in Girdin ncKO mice.

3.4. Measurement of mRNA of Girdin, hypothalamic genes and the IGF-I gene

The growth retardation of cKO mice appears shortly after birth. This fact suggests that loss of Girdin function in neuronal lineages produces lethality; however, a number of mouse models that also display hypoplasia of the OB, or GCD in the dentate gyrus, are viable. Thus, it seems likely that other unknown abnormalities are the cause of death in the Girdin cKO mouse. Because the hypothalamus is a key regulator of body homeostasis by controlling food intake, metabolic rate, thermo-regulation, fluid balance, steroid regulation, and growth, we explored whether mis-regulation of genes that encode hypothalamic hormones underlies the phenotype of cKO mice. The physiological functions of the hypothalamus are mediated by several key neurohumoral factors: thyrotropin releasing hormone (TRH) for thermo-regulation [15,16], arginine vasopressin (AVP) for fluid balance [17], corticotropin releasing hormone (CRH) for steroid regulation [18], and growth hormone releasing hormone (GHRH) for growth [19]. Thus, we determined whether transcripts for *TRH*, *AVP*, *CRH* and *GHRH* were reduced in the brains of cKO mice. We also analyzed the expression of Insulin-like growth factor-I (*IGF-I*), a downstream effector of GHRH in the liver. However, semi-quantitative RT-PCR analyses did not detect any significant reduction of mRNA expression in cKOs compared with other genotypes (Supplementary Fig. 5). These results indicate that the growth retardation and postnatal lethality observed in Girdin cKO mice are not due to altered expression of hypothalamic hormone genes.

4. Discussion

To determine which Girdin-positive tissues contribute most significantly to the phenotype of Girdin ncKO mice, we generated Girdin cKO mice. The phenotype of nestin-Cre-driven Girdin cKO mice were essentially identical to those of Girdin ncKO mice, including morphological abnormalities in the brain (OB hypoplasia with a widened RMS, and GCD in the dentate gyrus), growth retardation and postnatal lethality. Considering that nestin is a marker of pro-

liferating neural progenitor cells, we conclude that Girdin is essential for proper development and/or maintenance of the neuronal populations that exhibited abnormalities in Girdin KO mice. The results of chi-square tests between observed birth rates and expected Mendelian rates do not indicate embryonic lethality in either Girdin ncKO mice or Girdin cKO mice. This fact suggests that Girdin is more important for survival postnatally than prenatally.

Since there are several viable mouse models with hypoplasia of the OB (e.g. N-CAM deficient mice) [20] or with GCD of the dentate gyrus (e.g. Reelin deficient mouse) [21], other unknown neural dysfunctions in Girdin cKO mice could cause the postnatal lethality. We hypothesized that malnutrition is the cause of death because postmortem analyses of Girdin cKO mice revealed a severely reduced fat composition. One possible defect that could lead to malnourishment is altered expression of hormones that regulate body homeostasis. Although Girdin-driven β-galactosidase activity was detected in various regions of the brain, the expression of mRNAs of hormones produced in the hypothalamus was not affected in Girdin cKO mice. Thus, it is possible that the postnatal growth retardation and pre-weaning lethality of Girdin cKO mice are caused by broader and more fundamental abnormalities within the nervous system.

In conclusion, loss of Girdin from the nestin cell lineage alone results in phenotype (postnatal lethality, postnatal growth retardation, OB hypoplasia, and GCD in the dentate gyrus) that are similar to those seen after germ-line deletion. Because Girdin is thought to be a hub protein that interacts with many other proteins [1,4,11,13,22], further detailed analyses are necessary to elucidate the physiological roles of Girdin and to characterize the phenotype observed in both the conditional and germ-line KO mice.

Acknowledgments

This work was supported by a Grant-in-Aid for Global Center of Excellence (GCOE) Research, Scientific Research (A), a Grant-in-Aid for Scientific Research on Innovative Areas (to MT).

Appendix A. Supplementary data

Supplementary data associated with this article can be found, in the online version, at http://dx.doi.org/10.1016/j.bbrc.2012.08.122.

References

[1] A. Enomoto, H. Murakami, N. Asai, N. Morone, T. Watanabe, K. Kawai, Y. Murakumo, J. Usukura, K. Kaibuchi, M. Takahashi, Akt/PKB regulates actin organization and cell motility via Girdin/APE, Dev. Cell 9 (2005) 389–402.

[2] T. Kitamura, N. Asai, A. Enomoto, K. Maeda, T. Kato, M. Ishida, P. Jiang, T. Watanabe, J. Usukura, T. Kondo, F. Costantini, T. Murohara, M. Takahashi, Regulation of VEGF-mediated angiogenesis by the Akt/PKB substrate Girdin, Nat. Cell Biol. 10 (2008) 329–337.

[3] P. Jiang, A. Enomoto, M. Jijiwa, T. Kato, T. Hasegawa, M. Ishida, T. Sato, N. Asai, Y. Murakumo, M. Takahashi, An actin–binding protein Girdin regulates the motility of breast cancer cells, Cancer Res. 68 (2008) 1310–1318.

[4] A. Enomoto, N. Asai, T. Namba, Y. Wang, T. Kato, M. Tanaka, H. Tatsumi, S. Taya, D. Tsuboi, K. Kuroda, N. Kaneko, K. Sawamoto, R. Miyamoto, M. Jijiwa, Y. Murakumo, M. Sokabe, T. Seki, K. Kaibuchi, M. Takahashi, Roles of disrupted-in-schizophrenia 1-interacting protein girdin in postnatal development of the dentate gyrus, Neuron 63 (2009) 774–787.

[5] Y. Wang, N. Kaneko, N. Asai, A. Enomoto, M. Isotani-Sakakibara, T. Kato, M. Asai, Y. Murakumo, H. Ota, T. Hikita, T. Namba, K. Kuroda, K. Kaibuchi, G.L. Ming, H. Song, K. Sawamoto, M. Takahashi, Girdin is an intrinsic regulator of neuroblast chain migration in the rostral migratory stream of the postnatal brain, J. Neurosci. 31 (2011) 8109–8122.

[6] C. Zhao, W. Deng, F.H. Gage, Mechanisms and functional implications of adult neurogenesis, Cell 132 (2008) 645–660.

[7] M.E. Hatten, New directions in neuronal migration, Science 297 (2002) 1660–1663.

[8] C.R. Houser, Granule cell dispersion in the dentate gyrus of humans with temporal lobe epilepsy, Brain Res. 535 (1990) 195–204.

[9] C.A. Haas, M. Frotscher, Reelin deficiency causes granule cell dispersion in epilepsy, Exp. Brain Res. 200 (2010) 141–149.

[10] C.G. Lobe, K.E. Koop, W. Kreppner, H. Lomeli, M. Gertsenstein, A. Nagy, Z/AP, a double reporter for cre-mediated recombination, Dev. Biol. 208 (1999) 281–292.

[11] F. Simpson, S. Martin, T.M. Evans, M. Kerr, D.E. James, R.G. Parton, R.D. Teasdale, C. Wicking, A novel hook-related protein family and the characterization of hook-related protein 1, Traffic 6 (2005) 442–458.

[12] M. Anai, N. Shojima, H. Katagiri, T. Ogihara, H. Sakoda, Y. Onishi, H. Ono, M. Fujishiro, Y. Fukushima, N. Horike, A. Viana, M. Kikuchi, N. Noguchi, S. Takahashi, K. Takata, Y. Oka, Y. Uchijima, H. Kurihara, T. Asano, A novel protein kinase B (PKB)/AKT-binding protein enhances PKB kinase activity and regulates DNA synthesis, J. Biol. Chem. 280 (2005) 18525–18535.

[13] H. Le-Niculescu, I. Niesman, T. Fischer, L. DeVries, M.G. Farquhar, Identification and characterization of GIV, a novel Galpha i/s-interacting protein found on COPI, endoplasmic reticulum–golgi transport vesicles, J. Biol. Chem. 280 (2005) 22012–22020.

[14] U. Lendahl, L.B. Zimmerman, R.D. McKay, CNS stem cells express a new class of intermediate filament protein, Cell 60 (1990) 585–595.

[15] J. Bøler, F. Enzmann, The identity of chemical and hormonal properties of the thyrotropin releasing hormone and pyroglutamyl-histidyl-proline amide, Biochem. Biophys. Res. Commun. 37 (1969) 705–710.

[16] R. Burgus, T.F. Dunn, D. Desiderio, R. Guillemin, Molecular structure of the hypothalamic hypophysiotropic TRF factor of ovine origin: mass spectrometry demonstration of the PCA-His-Pro-NH2 sequence, Comptes rendus hebdomadaires des séances de l'Académie des sciences Série D: Sciences naturelles 269 (1969) 1870.

[17] G. Oliver, E.A. Schafer, On the physiological action of extracts of pituitary body and certain other glandular organs: preliminary communication, J. Physiol. 18 (1895) 277–279.

[18] A.V. Schally, S. Sawano, A. Arimura, J.F. Barrett, I. Wakabayashi, C.Y. Bowers, Isolation of growth hormone-releasing hormone (GRH) from porcine hypothalami, Endocrinology 84 (1969) 1493–1506.

[19] R. Guillemin, P. Brazeau, P. Bohlen, F. Esch, N. Ling, W.B. Wehrenberg, Growth hormone-releasing factor from a human pancreatic tumor that caused acromegaly, Science 218 (1982) 585–587.

[20] H. Cremer, R. Lange, A. Christoph, M. Plomann, G. Vopper, J. Roes, R. Brown, S. Baldwin, P. Kraemer, S. Scheff, Inactivation of the N-CAM gene in mice results in size reduction of the olfactory bulb and deficits in spatial learning, Nature 367 (1994) 455–459.

[21] B.B. Stanfield, W.M. Cowan, The morphology of the hippocampus and dentate gyrus in normal and reeler mice, J. Comp. Neurol. 185 (1979) 393–422.

[22] K. Ohara, A. Enomoto, T. Kato, T. Hashimoto, M. Isotani-Sakakibara, N. Asai, M. Ishida-Takagishi, L. Weng, M. Nakayama, T. Watanabe, K. Kato, K. Kaibuchi, Y. Murakumo, Y. Hirooka, H. Goto, M. Takahashi, Involvement of Girdin in the determination of cell polarity during cell migration, PLoS One 7 (2012) e36681.